

A parallel workflow implementation for PEST version 13.6 in high-performance computing for WRF-Hydro version 5.0: a case study over the midwestern United States

¹Jiali Wang, ¹Cheng Wang, ²Vishwas Rao, ¹Andrew Orr, ¹Rao Kotamarthi

¹Argonne National Laboratory, Environmental Science Division, 9700 South Cass Avenue, Lemont, IL 60439, USA

²Argonne National Laboratory, Mathematics and Computer Science Division, 9700 South Cass Avenue, Lemont, IL 60439, USA

Correspondence to: Jiali Wang (jialiawang@anl.gov)

Abstract. The Weather Research and Forecasting Hydrological (WRF-Hydro) system is a state-of-the-art numerical model that models the entire hydrological cycle based on physical principles. As with other hydrological models, WRF-Hydro parameterizes many physical processes. Hence, WRF-Hydro needs to be calibrated to optimize its output with respect to observations for the application region. When applied to a relatively large domain, both WRF-Hydro simulations and calibrations require intensive computing resources and are best performed on multimode, multicore high-performance computing (HPC) systems. Typically, each physics-based model requires a calibration process that works specifically with that model and is not transferrable to a different process or model. The parameter estimation tool (PEST) is a flexible and generic calibration tool that can be used in principle to calibrate any of these models. In its existing configuration, however, PEST is not designed to work on the current generation of massively parallel HPC clusters. To address this issue, we ported the parallel PEST to HPCs and adapted it to work with WRF-Hydro. The porting involved writing scripts to modify the workflow for different workload managers and job schedulers, as well as developing code to connect parallel PEST to WRF-Hydro. To test the operational feasibility and the potential computational benefits of this first-of-its-kind HPC-enabled parallel PEST, we developed a case study using a flood in the midwestern United States in 2013. Results on a problem involving calibration of 22 parameters show that on the same computing resource used for parallel WRF-Hydro, the HPC-enabled parallel PEST can speed the calibration process by a factor of up to 15 compared with commonly used

1 PEST in sequential mode. The speedup factor is expected to be greater with a larger calibration
2 problem (e.g., more parameters to be calibrated or a larger size of study area).

3 **1 Introduction**

4 Physically based hydrological models contain detailed physical mechanisms to model the
5 hydrological cycle, but many complex physical processes in these models are parameterized. For
6 example, the state-of-the-art Weather Research and Forecasting Hydrological (WRF-Hydro)
7 modeling system (Gochis et al., 2015) has dozens of parameters that can be land- and river-type
8 dependent and are typically specified in lookup tables. Therefore, these hydrological models need
9 to be calibrated before they can be applied to research over different regions. In this context,
10 calibration refers to adjusting the values of the model parameters so that the model can closely
11 match the behavior of the real system it represents. In some cases, the appropriate value for a
12 model parameter can be determined through direct measurements conducted on the real system. In
13 many situations, however, the model parameters are conceptual representations of abstract
14 watershed characteristics and must be determined through calibration. In fact, model calibration is
15 the most time-consuming step, not only for hydrological models, but also for Earth system model
16 development, because both parametric estimation and parametric uncertainty analysis require
17 hundreds—if not thousands—of model simulations to understand how perturbations in model
18 parameters affect simulations of dominant physical processes and to find the optimum value of a
19 single parameter.

20
21 WRF-Hydro is a numerical model that can simulate the entire hydrological cycle using advanced
22 high-resolution data such as satellite and radar products. Compared with the traditional land
23 surface model (LSM) used by WRF, WRF-Hydro provides a framework for multiscale
24 representation of surface flow, subsurface flow, channel routing, and baseflow, as well as a simple
25 lake/reservoir routing scheme. As a physics-based model, WRF-Hydro includes many complicated
26 physical processes that are nonlinear and must be parameterized. The default parameters given by
27 WRF-Hydro may be valid for one region but not for another region. Hence calibration of related
28 model parameters is often required in order to use the model in a new domain. In particular, for a
29 large spatial domain such as the entire contiguous United States, in order to develop the optimal
30 parameter sets in a reasonable amount of time, the calibration must be conducted on high-

1 performance computing (HPC) systems in parallel instead of in the traditional sequential mode.
2 To date, no such calibration tool can efficiently calibrate WRF-Hydro on HPC resources.
3 Typically, each physics-based model needs a calibration code that is custom designed to work with
4 that particular numerical model and its set of physics parameterizations, software architecture, and
5 solvers. These custom-designed calibration codes are highly challenging and do not offer
6 flexibility. Therefore, a more flexible and generic calibration tool is needed that can calibrate any
7 code that uses Message Passing Interface/Open Multi Processing (MPI/OpenMP) for
8 parallelization on HPC systems.

9
10 One widely used generic and independent calibration tool is the parameter estimation tool (PEST).
11 PEST (Doherty, 2016) conducts calibration automatically based on mathematical methods and
12 thus is applicable for optimizing nonlinear parameters. Compared with manual calibration,
13 automatic calibration is more efficient and effective because it avoids interference from human
14 factors (Madsen, 2000; Getirana, 2010). The uniqueness of PEST is that it operates independent
15 of models: there is no need to develop additional programs or codes for a particular model except
16 preparing the files required by PEST (as described in Sec. 3.2). PEST has four modes of operation.
17 One of the modes is regularization mode, which supports the use of Tikhonov regularization and
18 is found better for serving environmental models because, if implemented properly, it supports
19 model predictions of minimum error variance, is numerically stable, and embraces rather than
20 eschews the heterogeneity of natural systems. Singular value decomposition (SVD) can be used as
21 a regularization device to guarantee numerical stability of the calibration problem. Parallel PEST
22 is able to distribute many runs across many computing nodes using master-worker parallel
23 programming. To our best knowledge, however, no approach is available that allows users to submit
24 jobs using PEST parallelization to a typical supercomputing facility that uses job scheduling and
25 workload management such as Simple Linux Utility for Resource Management (SLURM),
26 Portable Batch System (PBS), and Cobalt. A previous study (Senatore et al., 2015) used PEST to
27 calibrate WRF-Hydro over the Crati River Basin in southern Italy. Because the study area was
28 relatively small, the authors were able to conduct the calibration using PEST in sequential mode
29 (Alfonso Senatore, personal communication, 2018).

30

1 This study aims to (1) port parallel PEST to HPC clusters operated by the U.S. Department of
2 Energy (DOE) and adapt it to work with WRF-Hydro, (2) evaluate the performance of HPC-
3 enabled parallel PEST linked to WRF-Hydro by calibrating a flood event, and (3) explore the
4 scale-up capability and computational benefits of HPC-enabled parallel PEST by assigning
5 different computing resource to the entire calibration process.

6 **2 Model description**

7 **2.1 Study area**

8 The case presented here is one of the worst floods experienced by greater Chicago area in the past
9 three decades; the storm occurred on April 18, 2013 (Campos and Wang, 2015). According to the
10 National Weather Service (NWS), the heaviest 24-hour accumulated rainfall during this storm
11 reached 201.4, 171.1, and 136.4 mm across Illinois, Iowa, and Missouri, respectively. The
12 Mississippi River crested at 10.8 m (1.7 m above flood stage), and the Illinois River crested in
13 Peoria, Illinois, at 8.95 m; these river cresting broke the previous record of 8.78 m, set in 1943,
14 and was 4.55 m above the historical normal river stage (NWS, 2013). Campos and Wang (2015)
15 conducted three-domain nested WRF simulations to understand the dynamical and microphysical
16 mechanisms of the event. Our study builds on the smallest domain of that study, which covers the
17 majority of Illinois, Iowa, and Missouri at a spatial resolution of 3 km (Fig. 1). The domain size is
18 750 km from west to east and 660 km from south to north.

19

20 **2.2 WRF-Hydro configuration**

21 This study employs WRF-Hydro version 5 with a basic configuration. This configuration does not
22 use nudging techniques or spatially distributed soil-related parameters as used in the National
23 Water Model configuration. WRF-Hydro has been tested in several different cases that focused on
24 different hydrometeorological forecasting and simulation problems (e.g., Gochis et al., 2018;
25 Yucel et al., 2015; Senatore et al., 2015; Arnault et al., 2016), and it shows reasonable accuracy in
26 simulated streamflow after being carefully calibrated. For details of the WRF-Hydro modeling
27 system, see Gochis et al. (2018). Currently, two LSMs are available in WRF-Hydro for
28 representing land-surface column physics: Noah (Chen and Dudhia, 2001) and Noah Multi-

1 parameterization (Noah-MP; Niu et al. 2011). We utilize Noah-MP LSM because compared with
2 Noah LSM it shows obvious improvements in reproducing surface fluxes, skin temperature over
3 dry periods, snow water equivalent, snow depth, and runoff (Niu et al. 2011). The Noah-MP is
4 configured at a grid spacing of 3 km, and the aggregation factor is 15; that is, starting from a 3 km
5 LSM resolution in the domain shown in Fig. 1, hydrological routing is performed at a grid
6 resolution of 200 m, with 3285 south-north \times 3735 west-east grid cells. We use a time step of 10
7 seconds for the routing grid in order to maintain model stability and prevent numerical dispersion
8 of overland flood waves. The time step also meets the Courant condition criteria for diffusive wave
9 routing on a 200 m resolution grid. The WRF-Hydro is configured to be in offline or uncoupled
10 mode—there is no online interaction between the WRF-Hydro hydrological model and the WRF
11 atmospheric model. Overland flow, saturated subsurface flow, gridded channel routing, and a
12 conceptual baseflow are active in this study. The gridded channel network uses an explicit, one-
13 dimensional, variable time-stepping diffusive wave. A direct output-equals-input “pass-through”
14 relationship is adopted to estimate the baseflow. Although the baseflow module is not physically
15 explicit, it is important because the water flow in the channel routing is contributed by both the
16 overland flow and baseflow. If the overland flow is active as it is in this study, it passes water
17 directly to the channel model. In this case the soil drainage is the only water resource flowing into
18 the baseflow buckets. However, if the overland flow is deactivated but channel routing is still
19 active, then WRF-Hydro collects excess surface infiltration water from the land model and passes
20 this water into the baseflow bucket. This bucket then contributes the water from both overland and
21 soil drainage to the channel flow. Therefore, the baseflow must be active if the overland flow is
22 switched off. This study does not consider lakes and reservoirs.

23

24 We use the geographic information system (GIS) tool (Sampson and Gochis, 2018) developed by
25 the WRF-Hydro team to delineate the stream channel network, open water (i.e., lake, reservoir,
26 and ocean) grid cells, and groundwater/baseflow basins. Meteorological input for the WRF-Hydro
27 model system includes hourly precipitation; near-surface air temperature, humidity, and wind
28 speed; incoming shortwave and longwave radiation; and surface pressure. In this study, the hourly
29 precipitation is from the National Centers for Environmental Prediction (NCEP) Stage IV analysis
30 at a spatial resolution of 4 km. The Stage IV data is based on combined radar and gauge data (Lin
31 and Mitchell, 2005; Prat and Nelson, 2015), and has been shown to be temporally well correlated

1 with high-quality measurements from individual gauges (see, e.g., Sapiano and Arkin, 2009; Prat
2 and Nelson, 2015). The other hourly meteorological inputs are from the second phase of the multi-
3 institution North American Land Data Assimilation System project, phase 2 (NLDAS-2) (Xia et
4 al., 2012a,b), at a spatial resolution of 12 km. NLDAS-2 is an offline data assimilation system
5 featuring uncoupled LSMs driven by observation-based atmospheric forcing.

6
7 During the 15-day period of this studied case, light to moderate rain occurred on April 8 through
8 11, 2013, followed by a relatively dry period from April 12 to 15. Then a heavy rain event began
9 on April 16 and peaked on April 18. The heaviest rain band moved east of the study area on April
10 19. The rainy event ended over the study area on April 20 (see Fig. S1 in Supporting Information).
11 We start the WRF-Hydro simulation on Jan. 1, 2013, and run the model for more than three months
12 to reach equilibrium. This 3-month period is considered as spin-up time and is excluded from
13 model calibration and evaluation. We calibrate the river discharge calculated by the WRF-Hydro
14 model from 00UTC April 9 to 00UTC April 12, 2013, considering it long enough to achieve our
15 objective. We then evaluate the model performance against U.S. Geological Survey (USGS)
16 observed river discharge from 00UTC April 12 to 00UTC April 25, 2013.

17 **3 Calibration**

18 **3.1 Platforms**

19 We customized parallel PEST to work on three different workload managers and job schedulers:
20 SLURM at the National Energy Research Scientific Computing Center (NERSC), PBS at the
21 Argonne National Laboratory Computing Resource Center, and Cobalt at the Argonne Leadership
22 Computing Facility. The tests presented here are conducted on Edison at NERSC, which uses the
23 SLURM workload manager and job scheduler. Edison is a Cray XC30 with a peak performance
24 of 2.57 petaflops per second, 133,824 compute cores, 357 terabytes of memory, and 7.56 petabytes
25 of disk storage. It has 5,586 nodes and 24 cores per node.

26
27 The interface we have built between parallel PEST and the management software (SLURM here)
28 is, in general, used for (1) setting the number of workers and the nodes for each worker to conduct
29 a model run (WRF-Hydro here); (2) finding the nodes that are available; (3) setting up the working

1 directory for the workers; (4) identifying the nodes that work for each worker; (5) passing the
2 global files (same for all the working directory) to all the workers (these files include the lookup
3 table files that are not to be calibrated, the namelist files for both LSM and hydrological sector,
4 and restart files that generated by the previous simulations, or spin-up period); and (6) submitting
5 the job for the entire calibration process, including parallel PEST and parallel WRF-hydro. This
6 job can be submitted as a cold-start run or as a restart. The main difference for this interface on
7 different management software is that different management software has its own way to submit
8 jobs and identify available nodes. This difference requires some changes in the script we
9 developed.

10 **3.2 PEST files and settings**

11 PEST requires three file types in both sequential and parallel mode. They are template files to
12 define the parameters to be calibrated, an instruction file to define the format of model-generated
13 output files, and a control file to supply PEST with the size of the problem and the settings for the
14 calibration method. Parallel PEST uses a “master-worker” paradigm that starts model runs
15 simultaneously by different workers (or in different folders). The master of parallel PEST
16 communicates with each of its workers many times during a calibration. To run PEST in parallel
17 mode, one also needs a management file to inform PEST where the working folder is for each
18 worker and what the names and paths are for each model input file that PEST must write (i.e.,
19 lookup tables that come from template files) and each model output file that PEST must read (such
20 as frsxt_pts_out.txt). The management file also set the maximum running time for each worker.
21 For those workers that take longer than the maximum running time, PEST will stop the model run
22 by that particular worker and assign that model run to another worker if there is one with nothing
23 else to do.

24
25 To the best of our knowledge, however, parallel PEST is not designed to run on HPCs directly.
26 We developed scripts and an interface to enable parallel PEST to run on HPCs using SLURM,
27 PBS, or Cobalt workload managers and job schedulers. The development involved writing scripts
28 to modify the workflow for different workload managers and job schedulers, as well as developing
29 code to connect parallel PEST to WRF-Hydro. These developments enable parallel PEST to run
30 many workers at the same time; each worker runs a parallel code (here WRF-Hydro) that uses

1 more than one node, which could significantly reduce the wall-clock time of model calibrations.
2 Although this master-worker parallelism may not be as efficient as a fully MPI approach, it is
3 sufficient for model calibration and requires the least effort for the current parallel PEST to run on
4 HPC systems.

5
6 This study presents calibration results from PEST using the SVD-based regularization in
7 regularization mode to ensure numerical stability (Tonkin and Doherty, 2005). We focus on
8 calibrating 22 parameters (see Table 1 and detail description in Sec. 3.3) using 96 observation
9 points and 22 items of prior information for the calibrated parameters. In each item of prior
10 information, a value equal to its default value provided by the WRF-Hydro v5.0 (or the log of its
11 default value) is assigned for each adjustable parameter, assuming that default values are the
12 preferred values. All prior information equations are assigned a weight of 1.0. We assigned five
13 different regularization groups to the prior information: Manning’s roughness coefficients
14 specified by Strahler stream order in CHANPARAM.TBL to one group; the parameters in
15 HYDRO.TBL (Manning’s roughness coefficients for overland flow as a function of vegetation
16 types) to another group; and three global parameters for the Noah-MP (xslop1, refdk, and refkdt)
17 in GENPARAM.TBL to the remaining three groups. The 96 observation points are given different
18 weights based on the inversed mean of their observed discharge during the studied period (see the
19 detailed description in Sec. 3.3 and Sec. 4.1). For a detailed description of these settings see the
20 PEST User Manual (Doherty, 2016).

21

22 **3.3 Calibrated experiments**

23 The primary objective of this study is to build a bridge for linking the parallel PEST and WRF-
24 hydro on the basis of HPC clusters and to explore the computational benefits of this bridge. We
25 do not attempt to extensively assess each individual tool or address questions in each individual
26 domain, such as optimizing the objective functions in PEST or calibrating WRF-Hydro for a long
27 time period considering all the relevant parameters to achieve an optimal parameter set. The
28 calibration period thus is limited to only three days, which we believe long enough to achieve our
29 objective and to understand WRF-Hydro’s sensitivity to the calibrated parameters. We calibrated
30 WRF-Hydro using four USGS sites (referred to as Station 1, Station 2, Station 3, and Station 4

1 hereafter), as shown in Fig. 1. (More USGS sites could be included if one manually reallocated
2 the stations that were not properly assigned to the desired location on the channel network by the
3 GIS tool.) We then transfer the calibrated parameters to other subbasins in the study area to assess
4 the transferability of the calibrated parameters. Although many parameters, including spatially
5 distributed parameters and constant parameters in the lookup tables, affect the model performance,
6 we calibrate only the parameters in lookup tables and do not consider the spatial variability of
7 other parameters or their scaling factors. We acknowledge that some studies calibrate a single
8 scaling factor (without considering its spatial variability, however) of overland roughness
9 coefficients (OVROUGHRTFAC) rather than the actual value of each land type in the lookup table
10 (e.g., Kerandi et al., 2018). Although this approach reduces the number of calibrated parameters,
11 however, it has less flexibility because changing one factor will change all the parameters that use
12 the same proportion.

13

14 For the calibration exercises we conduct here, the retention depth factor (RETDEPRTFAC) is
15 fixed at 0.001. This value is reasonable because the modeled discharge of our particular
16 configuration (Sec. 2.2) using default parameters is lower than observed discharge. Reducing this
17 factor from 1 to 0.001 keeps less water in water ponds and more water on the surface so it can
18 contribute to river discharge. First, we calibrate 48 parameters based on a 3-day simulation from
19 April 9 to April 11, 2013 (Table S1 in Supporting Information). This calibration uses the
20 estimation mode in the PEST tool and considers equal weight for all four USGS stations. We
21 calibrate Manning’s roughness coefficients for both channels and land-use types, the deep drainage
22 (SLOPE), infiltration-scaling parameter (REFKDT), and saturated soil lateral conductivity
23 (REFDK). Manning’s roughness coefficients control the hydrograph shape and the timing of the
24 peaks; the SLOPE, REFKDT, and REFDK control the total water volume. Second, based on the
25 knowledge we learn from the 48-parameter calibration (see details in Sec. 4.1), for the same 3-day
26 period, we reduce the number of calibrated parameters from 48 to 22 according to the sensitiveness
27 of the WRF-Hydro model to the adjustable parameters. For example, during the calibration we
28 find that Manning’s roughness coefficients for several land types barely change because these land
29 types (e.g., tundra, snow/ice) are not present in the study area. We also learn that even though the
30 calibrated WRF-Hydro parameters can generate discharge results that closely resemble
31 observations, the physical meaning of several parameters are not appropriate because of the wide

1 range of those parameters that we set in the PEST control file. For example, Manning’s roughness
 2 coefficient for stream order 1 (0.199) is calibrated smaller than that for stream order 2 (0.218); the
 3 overland roughness coefficients for evergreen needleleaf forest (0.043) and mixed forest (0.023)
 4 are calibrated smaller than for cropland/woodland (0.046). Neither of these is true in the real world.
 5 We therefore adjust the range of many parameters according to the literature (Soong et al., 2012)
 6 to maintain their physical meanings (Table 1). We find that by using the same absolute weight for
 7 all four stations, the calibration helps three stations (Station 2, 3, and 4) with large water volumes
 8 to generate more reasonable results than do the default parameters; however, the results for Station
 9 1, which has a relatively small volume of water, is not always better than the discharge that is
 10 modeled by using default parameters. Thus, we assign a weight of 15.0 for Station 1 versus a
 11 weight of 1.0 for the other three stations according to the inversed mean of observed discharge
 12 over these four stations in April 2013. The ratio of the weights between Station 1 and the other
 13 three stations stays similar even if the means are calculated based on different time periods.

14

15 **3.4 Statistics**

16 This study employs three statistical criteria: Nash–Sutcliffe efficiency (NSE; Nash and Sutcliffe,
 17 1970; Moriasi et al., 2007), root-mean-square error (RMSE), and Pearson correlation coefficient
 18 (PCC). RMSE and PCC evaluate model performance in terms of bias and temporal variation. NSE
 19 quantitatively describes the accuracy of modeled discharge compared with the mean of the
 20 observed data. Equation (1) calculates the NSE with defined variables:

$$21 \quad NSE = 1 - \frac{\sum_{t=0}^n (Y_t^{obs} - Y_t^{sim})^2}{\sum_{t=0}^n (Y_t^{obs} - Y_{mean}^{obs})^2}, \quad (1)$$

22 where Y_t^{obs} is the t th observed value from USGS sites for river discharge, Y_t^{sim} is the t th
 23 simulated value from the WRF-Hydro output, Y_{mean}^{obs} is the temporal average of USGS observed
 24 discharge, and n is the total number of observation time points. An efficiency of 1 (NSE = 1)
 25 corresponds to a perfect match between modeled discharge and observed data. An efficiency of 0
 26 (NSE = 0) indicates that the model predictions are as accurate as the mean of the observed data.
 27 An efficiency below zero (NSE < 0) occurs when the model is worse than the observed mean.
 28 Essentially, the closer the NSE is to 1, the more accurate the model is.

1 **4 Results**

2 **4.1 WRF-Hydro calibration and validation**

3 Based on the knowledge we gained from the 48-parameter 3-day calibration, we adjust the range
4 of critical parameters in the PEST control file to main their physical meanings. For example, we
5 set Manning’s roughness coefficient larger for stream order 1 than for stream order 2. We also
6 adjust the parameter range of the overland roughness coefficient for multiple land covers, such as
7 forests. We exclude the parameters that WRF-Hydro is not sensitive to for this study, in order to
8 constrain the problem size considering the availability of computational resources. However, if the
9 studied area is much larger with more land types than the study area here, then there would be
10 more parameters to calibrate. Also, hundreds of constant parameters in the Noah-MP model could
11 affect the WRF-Hydro results (Cuntz et al. 2016) and can be calibrated. Both these situations
12 would increase the burden of WRF-Hydro calibration. We perform the same 3-day calibration
13 from April 9 to April 11, 2013. Figure 2 shows the results of the 3-day modeled discharge (in cubic
14 meters) using default and calibrated parameters after five iterations, as well as observed discharge.
15 The four stations are calibrated by considering different weights. Compared with the results
16 calibrated by using equal weights for all the stations, by giving a higher weight to Station 1 the
17 model bias over Station 1 is significantly reduced, with a higher NSE (0.87 with higher weight
18 versus 0.14 with equal weight) and lower RMSE (48.1 versus 123.6). Over Stations 2, 3, and 4,
19 which sit on rivers with relatively large water volumes, the modeled discharge using the default
20 parameter underestimates the streamflow by more than 65%. PEST detects this underestimation
21 and immediately adjusts the parameters and increases the modeled discharge during the first
22 iteration. After the third iteration, the difference in calibrated results between different iterations
23 is relatively small. We allow the PEST to conduct five iterations and use the parameters obtained
24 from the fifth iteration as our optimum parameters. As shown in Table 2, when the optimum
25 parameters are used, the modeled discharges are much closer to the observations compared with
26 the modeled results when the default parameters were used. The NSEs for the four stations
27 increased from 0.73 (Station 1), -54.4 (Station 2), 157.3 (Station 3) and -1316.9 (Station 4) to 0.87,
28 0.64, 0.05, and -58.78, respectively, being closer to 1. The RMSEs decreased from 69.3, 3925.2,
29 3981.3, and 4391.3 m³/sec to 48.1, 318.2, 308.7, and 934.6 m³/sec, respectively. Giving a lower
30 weight for the three large river stations does not change the calibration results much.

1
2 During the validation period, compared with the modeled discharge using default parameters, as
3 shown in Table 2, the NSEs for all four stations are increased to be closer to 1; RMSEs are
4 decreased by 50% or more; and the correlation coefficients between the observed and modeled
5 discharge are increased from 0.8, 0.76, 0.21, and 0.72 to 0.98, 0.82, 0.80, and 0.75. Compared with
6 the results of calibration using the estimation mode (no regularization) in PEST, the SVD-based
7 regularization generates slightly better hydrograph shape with 24-hour later discharge peaks that
8 are closer to the observations. However, a problem remains with the hydrograph shapes of the
9 modeled discharge, especially with the modeled peak of discharge. For Station 1, the WRF-Hydro
10 almost captures the timing of the peak of discharge, although it still underestimates the water
11 volume by ~25%. The reason is that this study uses a direct pass-through baseflow module, which
12 does not account for slow discharge and long-term storage of the baseflow. Therefore, the largest
13 contribution to river discharge is from precipitation, and groundwater does not contribute much
14 discharge to the channels in a long-term view, as is also true for the other three large river stations.
15 Different from Station 1, for the other three large river stations, the WRF-Hydro modeled
16 discharge increases soon after the peak of precipitation and reaches a peak on April 21, 2013,
17 which is much earlier than the observed peak of river discharge (near April 24). The reason is that
18 the water contributions for these stations are from a larger river basin (Mississippi River) than we
19 included in our current study area. Thus, when a heavy precipitation event occurs over the entire
20 river basin, there will be a significant lag time (especially at the lower part of the basin) between
21 the peak of precipitation amount and the peak of river discharge. For example, the precipitation
22 over the upper part of Mississippi River Basin (MRB) has a peak amount on April 18–19, but the
23 river discharge did not reach its peak until April 24. Because our studied area covers only half of
24 the MRB, the modeled river discharge has a shorter delay period after the peak of precipitation
25 than does the observed river discharge. Enlarging the study area to include the entire MRB may
26 improve this situation. Alternatively, calibrating and validating local rivers that are included in the
27 current study area may also reduce the bias in hydrograph shape compared to calibrating and
28 validating large rivers. On the other hand, the WRF-Hydro simulated river discharge decreases
29 soon after it reaches the peak and much earlier than the observed discharge. The reason is again
30 that the direct pass-through baseflow employed by this study does not account for slow discharge
31 and long-term storage of the baseflow. As a result, the contribution from the baseflow to the river

1 discharge in model simulations does not stay as long as in real situations. In the observations, the
2 river discharge decreases from the peak at a speed of $\sim 500 \text{ m}^3/\text{sec}$ per day, while the modeled river
3 discharge decreases from the peak at a speed of $\sim 1667 \text{ m}^3/\text{sec}$ per day. Using exponential storage-
4 discharge function for the baseflow may improve this situation.

5

6 **4.2 Computational benefits of parallel PEST on HPCs**

7 The ability to scale up the calibration of WRF-Hydro by using parallel PEST on HPC systems is
8 determined by two factors: the scale-up capability of parallel PEST and the scale-up capability of
9 WRF-Hydro. In calibrating WRF-Hydro, PEST first makes as many model runs as there are
10 adjustable parameters to calculate Jacobian matrix (Doherty, 2016). The Jacobian matrix has a
11 column for each calibrated parameter and a row for each observation and each item of prior
12 information that set in the PEST control file. These model runs are independent between workers
13 and can be easily parallelized. Each worker runs the model with temporarily incremented
14 parameters that are defined in the template and control files. Then, PEST needs to make additional
15 model runs to test parameter updates. Different from the Jacobian runs, these additional runs are
16 performed by using different Marquardt lambdas, and the search for a Marquardt lambda that
17 achieves the best set of parameters is a serial iterative process. The lambda to use for the next run
18 depends on the outcome of the model run conducted using the previously chosen lambda. Although
19 serial testing of Marquardt lambdas may quickly find the optimal Marquardt lambda in the first or
20 second series of model runs, it is an inefficient use of computing resources because other
21 processors are idle while only one process is searching the lambdas. This is especially true when
22 the model domain is large and requires extensive computing resources. This study employs “partial
23 parallelization” for the lambda-testing procedure (Doherty, 2016), so multiple workers can be used
24 to calculate parameter upgrades based on a series of lambda values that are related to each other
25 by a factor of RLAMFAC set in the PEST control file. We also set the value of PARLAM to -9999
26 in the management file so only one cycle of parallel WRF-hydro runs is devoted to testing
27 Marquardt lambdas. For additional details on these parameters and their settings see the PEST
28 User Manual (Doherty, 2016).

29

1 In this study we test the computational performance of HPC-enabled parallel PEST using different
2 number of workers (6, 12, and 23) for the 22-parameter calibration. As shown in Table 3, we
3 conducted five experiments: Test 1 uses 23 workers, Test 2 uses 12 workers, and Test 3 uses 6
4 workers. All three tests use two nodes for each worker to run WRF-Hydro in parallel. The
5 maximum number of lambda-testing runs undertaken per iteration is set to 15, 10, and 5 for Test
6 1, 2, and 3, respectively, to make sure that only one cycle of WRF-hydro runs is devoted (using
7 15, 10 and 5 workers from Tests 1, 2, and 3, respectively) to testing Marquardt lambdas. Note that
8 the maximum number of lambda-testing runs should be set equal to or less than the workers
9 available. Otherwise, another cycle of WRF-hydro runs needs to be conducted. In fact, generating
10 more Marquardt lambdas does not always guarantee that the best Marquardt lambdas are
11 generated. In contrast, it may make the model convergence slower (here, PEST) or even model
12 failure.

13

14 In order to test the trade-offs between the computing nodes used for running parallel WRF-Hydro
15 and the workers used for running parallel PEST, Tests 4 and 5 use different number of nodes for
16 each worker to run WRF-Hydro in parallel. Explicitly, Test 4 uses four nodes per worker, and Test
17 5 uses six nodes per worker. Both tests use six workers for running the parallel PEST. The
18 maximum number of lambda-testing runs undertaken per iteration is set to five for both Tests 4
19 and 5. Note that the time costs in Table 3 are limited to only one iteration. Conducting more
20 iterations will increase the cost of wall-clock time and computing, but will not change the
21 conclusion for the scale-up capability and computational benefits for HPC-enabled parallel PEST
22 linked to WRF-hydro.

23

24 PEST needs to run the WRF-Hydro model at least as many times as the number of calibrated
25 parameters (22 here). In fact, PEST runs the model 23 times in the first round (or the first iteration)
26 with initial parameter values and for the first Jacobian matrix. From the second iteration, it runs
27 the model 22 times to calculate Jacobian matrix. Therefore, if there are fewer than 23 workers, the
28 time cost for the first round of Jacobian matrix calculation will increase accordingly. For example,
29 as shown in Fig. 4a, when we assign 12 (and 6) workers to parallel PEST, the time cost for
30 calculating the Jacobian matrix is increased by a factor of 2 (and 4) compared with the time cost
31 of using 23 workers. The time cost for the parameter upgrade stays similar for the three

1 experiments because only one cycle of WRF-hydro simulation is conducted to test the Marquardt
2 lambdas. As a result, the total time cost for Test 2 is ~1.5 times more than that for Test 1, and the
3 total time cost for Test 3 is ~1.5 times more than that for Test 2 (Fig. 4b). By extrapolating the
4 speedup curve shown in Fig. 4a and Fig. 4b, we expect the total time cost to be ~1516 minutes
5 when using only one worker (or sequential mode), which is about 15 times slower compared with
6 running the PEST in parallel mode using 23 workers. For this particular study with 22 adjustable
7 parameters, we expect the time cost most likely to stay the same even if one increases the number
8 of workers to more than 23, because PEST runs WRF-Hydro only 23 or 22 times for each iteration.
9 Assigning more workers for this particular study would most likely render some workers idle and
10 is not an efficient use of computing resources. PEST may run WRF-Hydro more than 22 times
11 (e.g., 44 times) if higher-order finite differences are employed. In this case, assigning more
12 workers (e.g. 45 workers) may further speed up the calibration process. On the other hand, for the
13 same case study and using the same number of nodes for running parallel WRF-Hydro, we can
14 estimate the computing speedup by assuming an increase in the number of calibrated parameters
15 to 50. This would be the case, for example, to evaluate model sensitiveness to the physics in Noah-
16 MP or the spatial variabilities of certain parameters. We then expect to use 51 workers to achieve
17 the best computing performance for parallel PEST. This would then be 28–30 times faster than
18 running PEST using one worker (or in sequential mode). Similarly, if 100 parameters were used
19 for the calibration for the same case study, a factor of up to 60 speedup in the calibration process
20 would be achieved by running HPC-enabled parallel PEST.

21
22 In addition, by increasing the number of nodes for each worker to conduct WRF-Hydro (Tests 3,
23 4, and 5), the time cost for the entire calibration process is significantly reduced (Figs. 4c and 4d).
24 Specifically, the WRF-hydro scales up well when using four and six nodes compared with using
25 two nodes per worker for running the WRF-Hydro. Both the time spent on calculating the Jacobian
26 matrix and the time spent on testing the parameter upgrades are decreased by 49% and 67%,
27 respectively, when using four and six nodes. Therefore, the total time spent is also decreased when
28 using more nodes for each worker (see Table 3). Increasing the number of nodes to eight for each
29 worker will most likely further decrease the time cost by 70–75% compared with using only two
30 nodes per worker. Moreover, if one has a larger study area such as the entire contiguous United
31 States, we expect the WRF-Hydro to have an even better scale-up capability (e.g., on dozens of

1 nodes) than this study. Overall, based on the experiments we conduct here, using 23 workers for
2 parallel PEST and six nodes for each worker to run parallel WRF-Hydro would cost the least wall-
3 clock time—about 32 min for one iteration for this particular study.
4

5 **4.3 Evaluation of spatial transferability of the calibrated parameters**

6 To assess the transferability of the calibrated parameters, we apply the optimum parameters
7 obtained from the calibration for the four stations (black circles) in Fig. 1 to another set of four
8 stations (crosses in Fig. 1) in the study area. All four sites are located on relatively small rivers, so
9 the lag time between precipitation peak and the discharge peak are much shorter than that for the
10 stations on the lower part of MRB (e.g., Stations 2, 3, and 4). The assessment compares the
11 observed discharge with the closest grid cells from the discharge output of WRF-Hydro. Figure 5
12 shows the observed and modeled discharge using default and the optimum parameters. Overall,
13 WRF-Hydro’s default parameters underestimate the discharge and misrepresent the timing of
14 discharge peaks compared with observations over the four assessed stations (Stations 5, 6, 7, and
15 8). By using the calibrated parameters from other sites over the area, the model results increase the
16 discharge and shift the hydrograph shape so they are much closer to the observations than model
17 results using default parameters. The absolute error of simulated discharge decreases by 13.1%,
18 38.3%, and 71.6%, respectively, over Stations 6 through 8 (Station 5 shows a 6% increase of
19 absolute error), compared with the default simulated discharge. We also find that using the SVD-
20 based regularization for the PEST calibration captures the timing of discharge peak better than
21 using the estimation mode, which is one-day earlier than the observations reaching the discharge
22 peak.

23 **5 Summary and discussion**

24 WRF-Hydro is a new, and perhaps the first practical, computer code that can run on HPC systems
25 and can model the entire hydrological cycle using physics-based submodels and high-resolution
26 input datasets (e.g., radar). The hydrological community has desired this capability for decades,
27 although it requires intensive computing resources. Thus, the calibration of this model would
28 ideally be conducted on HPCs in parallel as well, especially when the model covers a large domain
29 rather than the basin scale. This study ports an independent model calibration tool, parallel PEST,

1 to HPC clusters and links it to WRF-Hydro to help WRF-Hydro users calibrate the model within
2 a much shorter wall-clock time period. The bridge we build here (between parallel PEST and
3 WRF-Hydro on the basis of HPC systems) can be applied to any other hydrological models and
4 Earth system models that use parameterizations to represent model physics. We present the
5 operational feasibility of the HPC-enabled parallel PEST by evaluating the performance of
6 calibrated WRF-Hydro against observation in hydrograph features such as volume and timing of
7 flood events. We examine the scale-up capability and computational benefits of the tool by
8 assigning different computing resource for PEST and for WRF-Hydro. While this study presents
9 the optimum parameters identified from the calibration of the particular flood event, the parameters
10 can be significantly different if one uses different physics, such as exponential storage-discharge
11 function for a groundwater model or reach-based channel routing. Our preliminary testing shows
12 that using exponential storage-discharge function with the default parameters provided by WRF-
13 Hydro, the modeled discharge was larger than that of observations. Thus, the calibration will need
14 to adjust the parameters to reduce the discharge. Our study finds that for calibrating 22 parameters,
15 using the same computing resource for running WRF-hydro, the HPC-enabled PEST calibration
16 tool can speed up WRF-Hydro calibration by a factor of 15, compared with running PEST in
17 sequential mode. The speedup factor can be larger when the number of parameters needing
18 calibration is higher (e.g., 50 or 100).

19

20 The following are several key points that we would like to mention to inform future studies:

- 21 1. In this study, we consider using the prior or regularization information only for the
22 parameters that we calibrate. As is the case with solving inverse problems, prior
23 information is added to improve the smoothness of the solutions. In order to build a more
24 comprehensive calibration, an important aspect that can be considered is to enrich the prior
25 with the available historical data. For example, in this particular case, one can use the
26 historical observation data (e.g., April and May from the past few years) to enrich the prior
27 information for the parameters. Hence, the regularization objective function in PEST will
28 constitute not only the discrepancies between parameters and their “current estimates” but
29 also the discrepancies between WRF-Hydro simulations and preferred values (which is the
30 observed time series of historical discharge). Additionally, one can use the pilot points
31 technique described by Doherty (2005) in conjunction with parameter estimation to add

1 more flexibility to the calibration process. This will be potentially beneficial in improving
2 the predictions.

- 3 2. To focus on our main goal, we calibrate only the parameters in lookup tables. However,
4 we acknowledge that using a single value to represent a physics for a large domain could
5 be problematic, especially we expect the HPC-enabled parallel PEST to execute with
6 WRF-Hydro for large domains. This situation often needs parameter regionalization. For
7 example, WRF-Hydro v5 has many spatially distributed parameters available, such as the
8 overland flow roughness scaling factor (OVROUGHRTFAC), the factor of maximum
9 retention depth (RETDEPRTFAC), and the soil-related parameters (when compiled with
10 SPATIAL_SOIL=1). Calibrating these spatial parameters based on grid scale (e.g.,
11 catchments) rather than a single value will give the model more flexibility and thus better
12 fit the observations (Hundecha and Bardossy, 2004; Wagener and Wheater, 2006). In
13 practice, for example, one can include regional OVROUGHRTFACs (e.g., their
14 lower/upper bounds, and default values) in the PEST control file based on catchments.
15 However, the selection of the locations and sizes of catchment may introduce significant
16 uncertainties to the calibration results, which require systematic and comprehensive
17 investigation and understanding of the study area.
- 18 3. This study is limited to calibrating the observed streamflow only based on the format of
19 one of WRF-Hydro model outputs for individual station or point (frxst_pts_out.txt). It is
20 feasible, however, to calibrate other variables as long as the observation data is available.
21 For example, one can either find the closest point from the gridded dataset to the
22 observation location and then compare that model grid to observations; or one can change
23 the WRF-Hydro input/output code to output other variables in the frxst_pts_out.txt file, so
24 they can still use the same interface we developed here to calibrate other variables instead
25 in addition to the discharge.
- 26 4. The optimal parameter set obtained from this study is from the 5th iteration of parallel
27 PEST by testing five Marquardt lambdas. Testing different number of lambdas or
28 calibrating different number of parameters may generate a different set of optimal
29 parameters. These parameter sets can all make physical sense and be equally good for
30 reproducing observed discharges. This problem is named equifinality (Beven and Freer,
31 2001; Savenije, 2001), which is an important source of model uncertainty. To reduce the

1 model uncertainty through reducing the equifinality, hydrologists carry out additional
2 modelling objective for model evaluation to find more useful parameter sets (Mo and
3 Beven, 2004; Gallart et al., 2007). Alternatively, inspired by No. 3 discussed above, one
4 can calibrate the WRF-hydro model based on more than one variables, such as discharge
5 and soil moisture (or heat flux or water table depth) to reduce the number of optimal
6 parameter sets, and thus reduce the model uncertainty of predictions for these variables.

- 7 5. While this study ported the parallel PEST to HPC system and linked it to WRF-Hydro, we
8 note that BEOPEST is available in the PEST family. BEOPEST has the same functionality
9 as parallel PEST but uses a different approach for communication between master and
10 workers. Working with HPC-enabled BEOPEST may save total time cost since BEOPEST
11 uses the Transmission Control Protocol (TCP) and the Internet Protocol (IP) instead of
12 message files (reading input and writing output between master and works) for
13 communication. We expect it to be relatively straightforward to use BEOPEST to calibrate
14 WRF-hydro on HPCs since the interface remains similar, except one needs to copy the
15 template and instruction files in addition to the global files (see Section 3.1) into each
16 working folder.

17
18 *Data and Code availability.* The observed river discharge is downloaded from the USGS Surface-
19 Water Data website, available at <https://waterdata.usgs.gov/nwis/sw>. The Stage IV precipitation
20 data were downloaded from <https://data.eol.ucar.edu/dataset/21.093>. PEST was downloaded from
21 <http://www.pesthomepage.org/Downloads.php>. We use the Unix PEST version 13.6. The scripts
22 and files that are developed in this study and required by PEST for calibrating WRF-Hydro are
23 available at <http://doi.org/10.5281/zenodo.2588506>.

24
25 *Author contributions.* JW proposed the project and developed the study case in WRF and WRF-
26 Hydro. CW developed the scripts/code to port the parallel PEST to DOE supercomputers and adapt
27 it to work with WRF-Hydro. VR provided important input for the regularization calibration
28 method. AO operated the ArcGIS tool to delineate the high-resolution grid cells to include stream
29 channel network, open water, and groundwater/baseflow basins. RK provide high-level guidance
30 and insight for the entire project. All authors commented on this manuscript.

31

1 *Competing interests.* The authors declare that they have no conflict of interest

2

3 *Acknowledgments.* This work is supported under a Laboratory Directed Research and
4 Development (LDRD) Program at Argonne National Laboratory, through U.S. Department of
5 Energy (DOE) contract DE-AC02-06CH11357. Computational resources are provided by the
6 DOE-supported National Energy Research Scientific Computing Center, Argonne National
7 Laboratory Computing Resource Center, and Argonne Leadership Computing Facility. Our special
8 thanks to the PEST developers and entire WRF-Hydro team, especially Kevin Sampson for his
9 guidance on the ArcGIS tool. We gratefully thank the two reviewers for their valuable comments
10 and suggestions, which tremendously improved this manuscript.

11 **References**

12 Arnault, J., Wagner, S., Rummler, T., Fersch, B., Bliefernicht, J., Andresen, S., and Kunstmann,
13 H.: Role of runoff–infiltration partitioning and resolved overland flow on land–atmosphere
14 feedbacks: A case study with the WRF-Hydro coupled modeling system for West Africa, *J.*
15 *Hydrometeorol.*, 17, 1489–1516, 2016.

16

17 Campos, E., and Wang, J.: Numerical simulation and analysis of the April 2013 Chicago Floods,
18 *J. Hydrol.*, 531, 454–474, 2015.

19

20 Chen, F. and Dudhia, J.: Coupling an advanced land surface-hydrology model with the Penn State-
21 NCAR MM5 modeling system, Part I: Model implementation and sensitivity, *Mon. Weather Rev.*,
22 129, 569–585, 2001.

23

24 Cuntz, M., Mai, J., Samaniego, L., Clark, M., Wulfmeyer, V., Branch, O., Attinger, S., and Thober,
25 S.: The impact of standard and hard-coded parameters on the hydrologic fluxes in the Noah-MP
26 land surface model, *J. Geophys. Res. Atmos.*, 121, 10,676–10,700, doi:10.1002/2016JD025097,
27 2016.

28

29 Doherty, J.: PEST: Model Independent Parameter Estimation, User Manual, 6th ed., Watermark
30 Numerical Computing, Brisbane, Queensland, Australia, 2016.

1
2 Doherty, J.: Ground water model calibration using pilot points and regularization, *Groundwater*,
3 41(2), 170–177, 2005.
4
5 Gallart, F., Latron, J., Llorens, P., and Beven, K. J.: Using internal catchment information to reduce
6 the uncertainty of discharge and baseflow predictions. *Adv. Water Resour.* 30(4), 808–823, 2007.
7
8 Getirana, A. C. V.: Integrating spatial altimetry data into the automatic calibration of hydrological
9 models, *J. Hydrol.*, 387 (3-4), 244–255, doi: 10.1016/j.jhydrol.2010.04.013, 2010.
10
11 Gochis, D. J., Barlage, M., Dugger, A., FitzGerald, K., Karsten, L., McAllister, M., McCreight, J.,
12 Mills, J., RafieeiNasab, A., Read, L., Sampson, K., Yates, D., and Yu, W.: The WRF-Hydro
13 modeling system technical description, (Version 5.0). NCAR Technical Note. 107 pages.
14 Available online at:
15 <https://ral.ucar.edu/sites/default/files/public/WRFHydroV5TechnicalDescription.pdf>, 2018.
16
17 Hundecha, Y., and Bárdossy, A.: Modeling of the effect of land use changes on the runoff
18 generation of a river basin through parameter regionalization of a watershed model, *J. Hydrol.*,
19 292, 281–295, 2004.
20
21 Kerandi, N., Arnault, J., Laux, P., Wagner, S., Kitheka, J., and Kunstmann, H.: Joint atmospheric-
22 terrestrial water balances for East Africa: A WRF-Hydro case study for the upper Tana River basin,
23 *Theor. Appl. Climatol.*, 131, 1337–1355, doi: 10.1007/s00704-017-2050-8, 2018.
24
25 Lin, Y., and Mitchell, K. E.: The NCEP stage II/IV hourly precipitation analyses: Development
26 and applications, Preprints, 19th Conf. on Hydrology, San Diego, CA, Amer. Meteor. Soc., 1.2.,
27 2005.
28
29 Madsen, H.: Automatic calibration of a conceptual rainfall–runoff model using multiple
30 objectives, *J. Hydrol.*, 235, 276–288, 2000.
31

1
2 Mo, X., and Beven, K.: Multi-objective parameter conditioning of a three-source wheat canopy
3 model. *Agricultural & Forest Meteorol.* 122(1–2), 39–63, 2004.
4 Moriasi, D. N., Arnold, J. G., Van Liew, M. W., Bingner, R. L., Harmel, R. D., and Veith, T. L.:
5 Model evaluation guidelines for systematic quantification of accuracy in watershed simulations,
6 *Transactions of the ASABE*, 50 (3), 885–900, 2007.
7
8 Nash, J. E., and Sutcliffe, J. V.: River flow forecasting through conceptual models, part I – A
9 discussion of principles, *J. Hydrol.*, 10(3), 282–290, doi: 10.1016/0022-1694(70)90255-6, 1970.
10
11 Niu, G.-Y., Yang, Z.-L., Mitchell, K. E., Chen, F., Ek, M. B., Barlage, M., Kumar, A., Manning,
12 K., Niyogi, D., Rosero, E., Tewari, M., and Xia, Y.: The community Noah land surface model with
13 multiparameterization options (Noah-MP): 1. Model description and evaluation with local-scale
14 measurements, *J. Geophys. Res.*, 116, D12109, doi: 10.1029/2010JD015139, 2011.
15
16 NWS (National Weather Service): Record river flooding of April 2013,
17 <https://www.weather.gov/ilx/apr2013flooding>, 2013.
18
19 Prat, O. P., and Nelson, B. R.: Evaluation of precipitation estimates over CONUS derived from
20 satellite, radar, and rain gauge data sets at daily to annual scales (2002-2012), *Hydrol. Earth Syst.*
21 *Sci.*, 19, 2037–2056, doi: 10.5194/hess-19-2037-2015, 2015.
22
23 Sampson, K., and Gochis, D.: WRF Hydro GIS Pre-processing tools, Version 5.0 Documentation,
24 2018.
25
26 Sapiano, M. R. P., and Arkin, P.A.: An intercomparison and validation of high-resolution satellite
27 precipitation estimates with 3-hourly gauge data, *J. Hydrometeorol.*, 10, 149–166, doi:
28 10.1175/2008JHM1052.1, 2009.
29
30 Senatore, A., Mendicino, G., Gochis, D. J., Yu, W., Yates, D. N., and Kunstmann, H.: Fully
31 coupled atmosphere-hydrology simulations for the central Mediterranean: Impact of enhanced

1 hydrological parameterization for short and long time scales, *J. Adv. Model. Earth Syst.*, 7(4),
2 1693–1715, doi: 10.1002/2015MS000510, 2015.

3

4 Soong, D. T., Prater, C. D., Halfar, T. M., and Wobig, L. A.: Manning’s roughness coefficients for
5 Illinois streams, U.S. Geological Survey Data Series 668, 2012.

6

7 Tonkin, M. J., and Doherty, J.: A hybrid regularized inversion methodology for highly
8 parameterized environmental models, *Water Resource Research*, 41, W10412,
9 doi:10.1029/2005WR003995, 2005.

10

11 Wagener, T., and Wheater, H. S.: Parameter estimation and regionalization for continuous
12 rainfall-runoff models including uncertainty, *J. Hydrol.*, 320, 132–154, 2006.

13

14 Xia, Y., Mitchell, K., Ek, M., Sheffield, J., Cosgrove, B., Wood, E., Luo, L., Alonge, C., Wei, H.,
15 Meng, J., Livneh, B., Lettenmaier, D., Koren, V., Duan, Q., Mo, K., Fan, Y., and Mocko, D.:
16 Continental-scale water and energy flux analysis and validation for the North American Land Data
17 Assimilation System project phase 2 (NLDAS-2), 1: Intercomparison and application of model
18 products, *J. Geophys. Res.*, 117, D03109, doi: 10.1029/2011JD016048, 2012a.

19

20 Xia, Y., Mitchell, K., Ek, M., Cosgrove, B., Sheffield, J., Luo, L., Alonge, C., Wei, H., Meng, J.,
21 Livneh, B., Duan, Q., and Lohmann, D.: Continental-scale water and energy flux analysis and
22 validation for the North American Land Data Assimilation System project phase 2 (NLDAS-2). 2.
23 Validation of model-simulated streamflow, *J. Geophys. Res.*, 117, D03110, doi:
24 10.1029/2011JD016051, 2012b.

25

26 Yucel, I., Onen, A. Yilmaz, K. K., and Gochis, D. J.: Calibration and evaluation of a flood
27 forecasting system: Utility of numerical weather prediction model, data assimilation and satellite-
28 based rainfall, *J. Hydrol.*, 523, 49–66, 2015.

1 **Table 1: Calibrated 22 parameters and the optimum parameters found after five iterations.**

Calibrated Parameter	Default	Lower Bound	Upper Bound	Optimum Parameter
mannn1	0.55	0.35	0.6	0.517599
mannn2	0.35	0.15	0.35	0.153894
mannn3	0.15	0.08	0.15	8.00E-02
mannn4	0.1	0.05	0.15	5.00E-02
mannn5	7.00E-02	0.02	0.1	6.677379E-02
mannn6	5.00E-02	0.015	0.1	1.628244E-02
mannn7	4.00E-02	0.01	0.08	1.298054E-02
mannn8	3.00E-02	0.005	0.06	5.00E-03
xslope1	0.1	1.00E-04	1	0.496680
refdk	2.00E-06	1.00E-08	1.00E-05	2.899043E-07
refkdt	1	0.01	5	1.66664
ovn1 (urban)	2.50E-02	0.005	0.06	6.00E-02
ovn2 (dry crop)	3.50E-02	0.015	0.06	1.50E-02
ovn3 (irrigated crop)	3.50E-02	0.015	0.06	1.50E-02
ovn5 (crop/grass)	3.50E-02	0.015	0.06	2.822497E-02
ovn6 (crop/wood)	6.80E-02	0.035	0.25	4.568903E-02
ovn7 (grass)	5.50E-02	0.015	0.25	1.50E-02
ovn10 (savanna)	5.50E-02	0.015	0.3	1.50E-02
ovn11 (deciduous forest)	0.2	0.1	0.3	0.30
ovn14 (evergreen forest)	0.2	0.1	0.3	0.164557
ovn15 (mixed forest)	0.2	0.1	0.3	0.112134
ovn16 (water)	5.00E-03	0.001	0.01	1.00E-02

1 **Table 2: Statistics of model performance using optimum and default (in parentheses)**
 2 **parameters for Stations 1–4 during the calibration and validation period.^a**

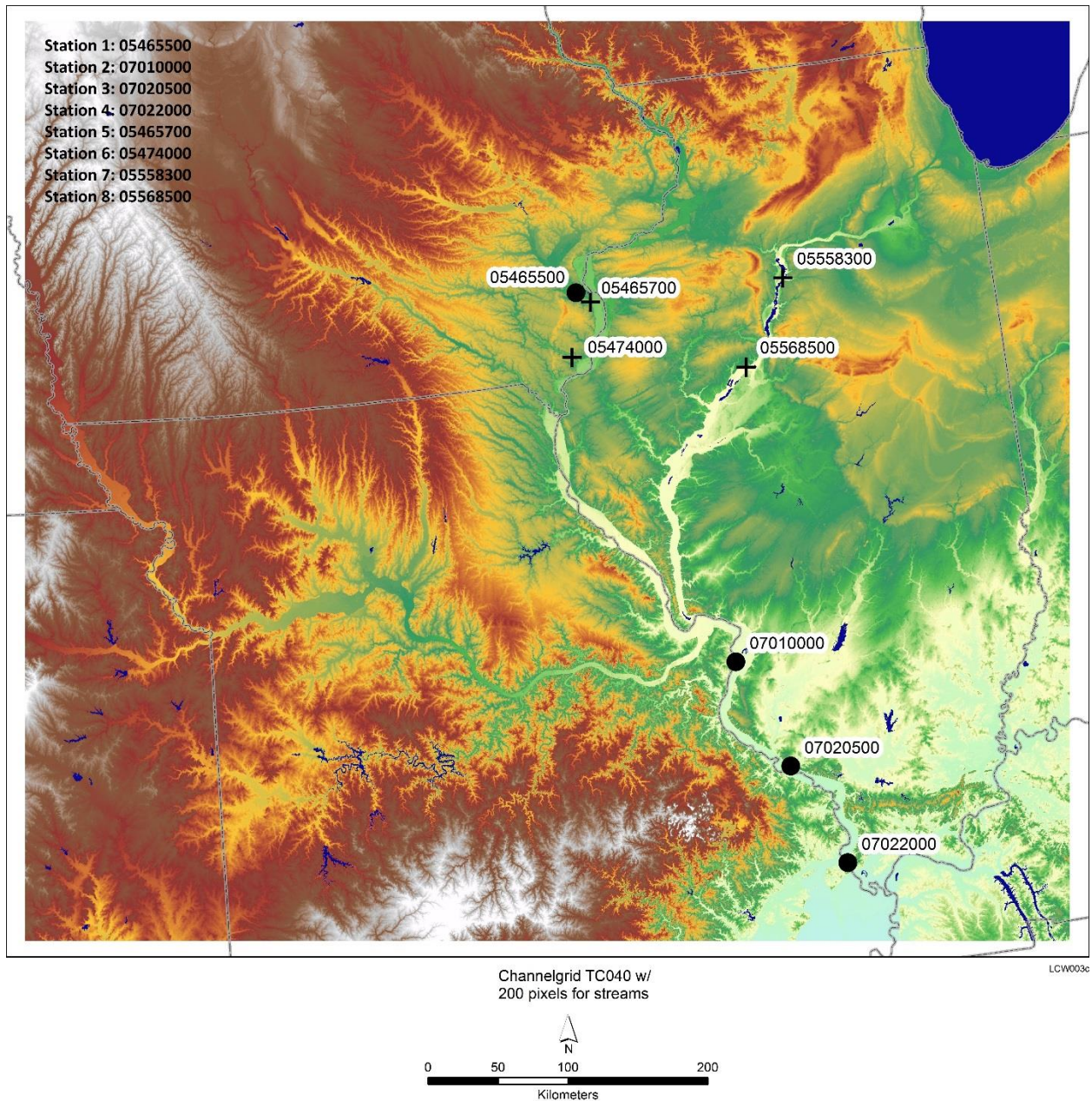
Statistics	Station 1	Station 2	Station 3	Station 4
Calibration				
NSE	0.87 (0.73)	0.64 (-54.4)	0.05 (-157.3)	-58.78 (-1316.9)
RMSE	48.1 (69.3)	318.2 (3925.2)	308.7 (3981.3)	934.6 (4391.3)
PCC	0.95 (0.91)	0.87 (0.92)	0.91 (0.87)	0.53 (0.66)
Validation				
NSE	0.83 (0.41)	-0.08 (-3.5)	-0.08 (-27.4)	-0.12 (-3.33)
RMSE	259.9 (487.3)	3264.3 (6670.1)	3170.1 (16305.7)	3283.9 (6854.3)
PCC	0.83 (0.8)	0.98 (0.69)	0.29 (0.19)	0.94 (0.64)

3 ^a The calibration period is 3 days (April 9–11) and includes 22 parameters. The validation period
 4 is April 12–24. Bold typeface indicates the calibrated model results are closer to observations
 5 compared with the default model results. NSE and PCC are unitless; RMSE is in m³/sec.

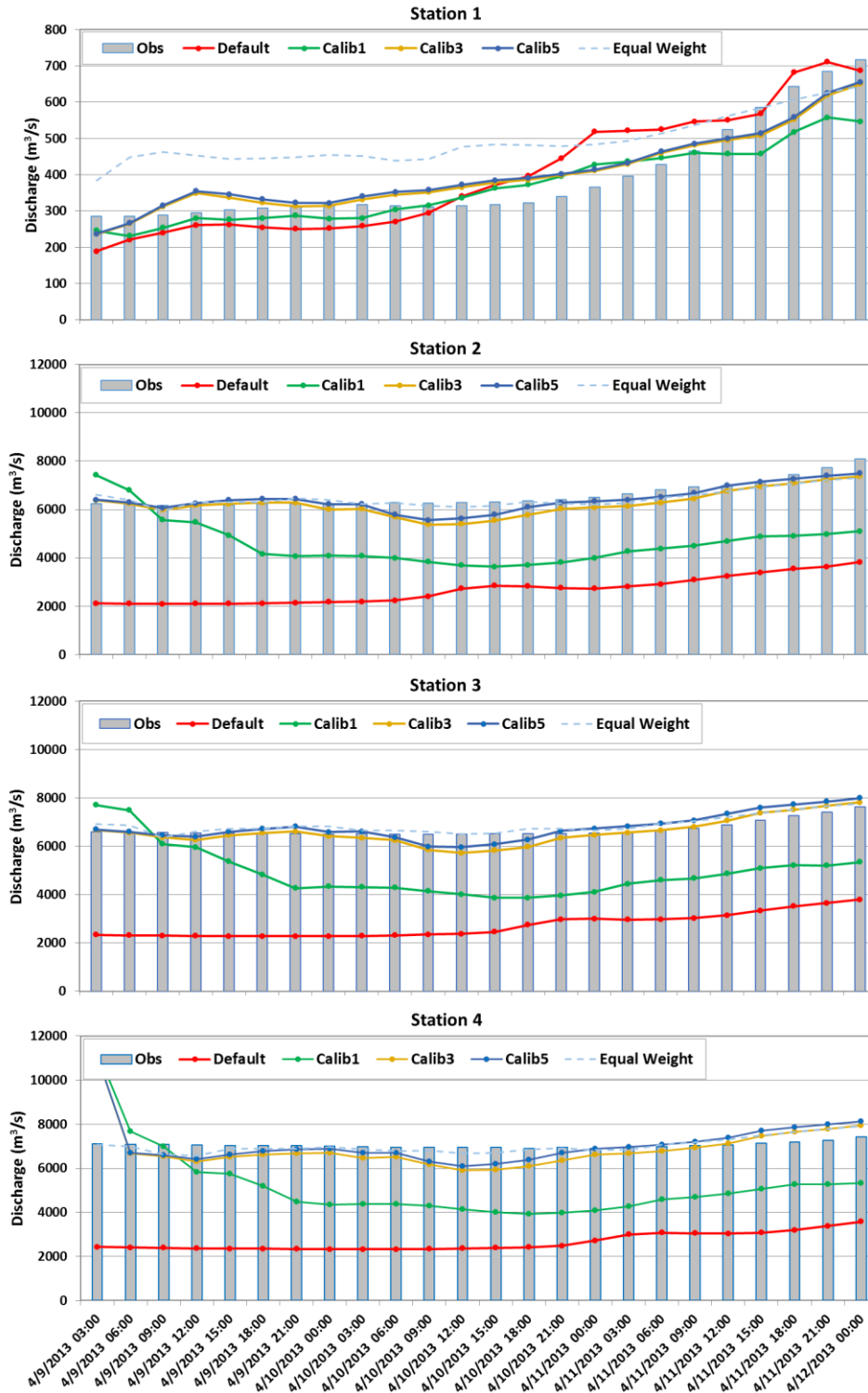
1 **Table 3. Experiments designed to test the scale-up capability and computational benefits of**
 2 **HPC-enabled parallel PEST linked to WRF-Hydro.**

Test	No. of Workers	No. of Lamdas	No. of Nodes for Each Worker	Total Time Cost (min)	Time Cost for Calculating Jacobian Matrix	Time Cost for Testing Parameter Upgrades
Test 1	23	15	2	103	52	51
Test 2	12	10	2	150	102	48
Test 3	6	5	2	264	211	53
Test 4	6	5	4	131	107	24
Test 5	6	5	6	86	70	16

3

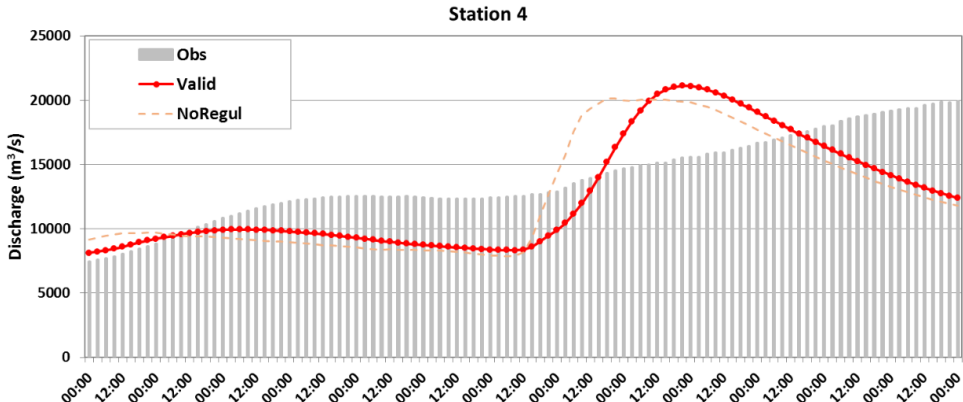
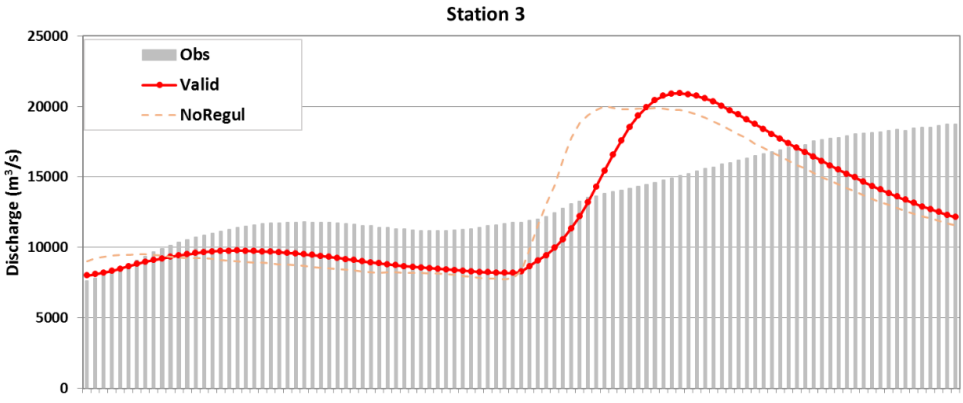
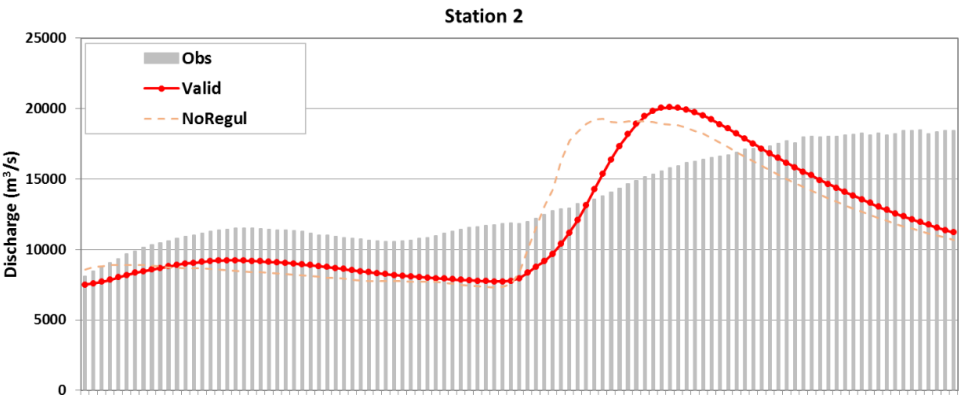
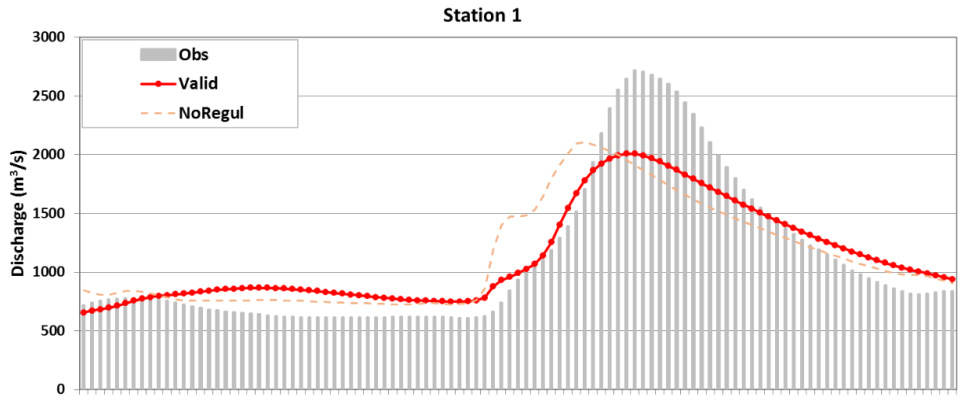


1
 2 **Figure 1: Eight USGS sites over the study area (750 km x 660 km). The four circles are sites**
 3 **that are used for calibrations; the four crosses are sites that are used for transferability**
 4 **assessment. USGS site numbers corresponding to the site index used in this study are listed**
 5 **on the top left corner of the map.**



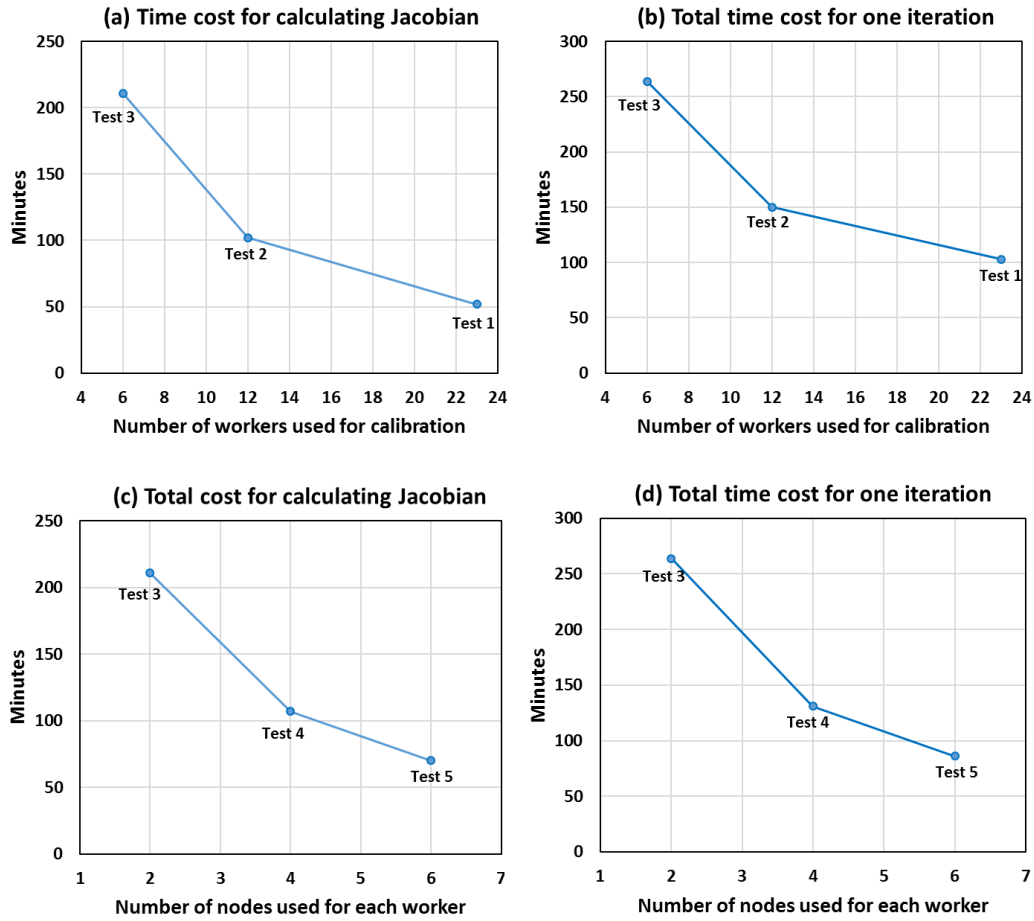
1
 2 **Figure 2: Observed and modeled discharge (m^3/sec) using default and calibrated parameters**
 3 **during a 3-day calibration period (April 9–11, 2013) over the four stations indicated by the**
 4 **black circles in Fig. 1. The calibrations shown in solid lines are conducted by using SVD-**

- 1 **based regularization and a higher weight for Station 1. The dashed line is the optimum result**
- 2 **calibrated by using equal weight for all four sites.**

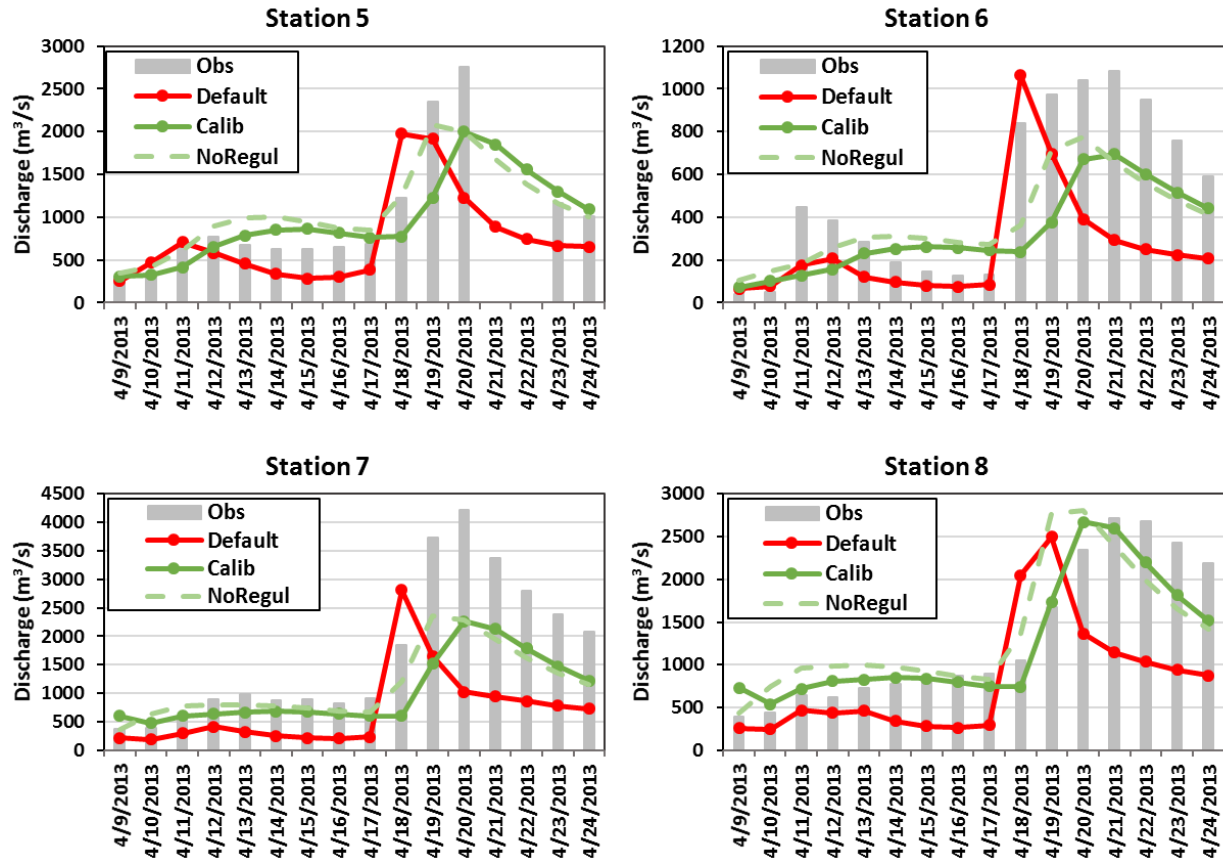


4/12/2013 00:00
 4/12/2013 12:00
 4/13/2013 00:00
 4/13/2013 12:00
 4/14/2013 00:00
 4/14/2013 12:00
 4/15/2013 00:00
 4/15/2013 12:00
 4/16/2013 00:00
 4/16/2013 12:00
 4/17/2013 00:00
 4/17/2013 12:00
 4/18/2013 00:00
 4/18/2013 12:00
 4/19/2013 00:00
 4/19/2013 12:00
 4/20/2013 00:00
 4/20/2013 12:00
 4/21/2013 00:00
 4/21/2013 12:00
 4/22/2013 00:00
 4/22/2013 12:00
 4/23/2013 00:00
 4/23/2013 12:00
 4/24/2013 00:00
 4/24/2013 12:00
 4/25/2013 00:00

1 **Figure 3: Observed and modeled discharge (m^3/sec) during a validation period (April 12–24,**
2 **2013) using optimum parameters identified from a 3-day calibration over the four stations**
3 **indicated by black circles in Fig. 1. The solid line uses the optimum parameters that**
4 **identified by PEST with SVD-based regularization and a higher weight for Station 1. The**
5 **dashed line uses the optimum result calibrated by using estimation mode (no regularization).**



1
 2 **Figure 4. Time cost for calculating Jacobian matrix and total time cost for one iteration for**
 3 **the five experiments (Table 3) using different number of workers to conduct PEST (a, b) and**
 4 **different number of nodes for each worker (c, d) to conduct WRF-Hydro.**



1
2 **Figure 5: Observed and modeled daily averaged discharge (m³/sec) from April 9–24 using**
3 **default and the optimum parameters (shown in Table 1) identified by the 3-day calibration**
4 **over four stations that are in the study area (indicated by crosses in Fig. 1). The calibrations**
5 **shown in solid lines are conducted by using SVD-based regularization and a higher weight**
6 **for Station 1. The dashed line is the optimum result calibrated by using estimation mode (no**
7 **regularization).**